



1 **Modelling winter organic aerosol at the European scale**
2 **with CAMx: evaluation and source apportionment with a**
3 **VBS parameterization based on novel wood burning smog**
4 **chamber experiments**

5 **Giancarlo Ciarelli¹, Sebnem Aksoyoglu¹, Imad El Haddad¹, Emily A. Bruns¹,**
6 **Monica Crippa², Laurent Poulain³, Mikko Äijälä⁴, Samara Carbone⁵, Evelyn**
7 **Freney⁶, Colin O'Dowd⁷, Urs Baltensperger¹ and André S. H. Prévôt¹**

8 [1]{Paul Scherrer Institute, Laboratory of Atmospheric Chemistry, 5232 Villigen PSI,
9 Switzerland}

10 [2]{European Commission, Joint Research Centre (JRC), Directorate for Energy, Transport
11 and Climate, Air and Climate Unit, Via E. Fermi 2749, I-21027 Ispra (VA), Italy}

12 [3]{Leibniz-Institute for Tropospheric Research (TROPOS), Permoserstr. 15, 04318 Leipzig,
13 Germany}

14 [4]{University of Helsinki, Department of Physics, Helsinki, Finland}

15 [5]{Institute of Physics, University of São Paulo, Rua do Matão Travessa R, 187, 05508-090
16 São Paulo, S.P., Brazil}

17 [6]{Laboratoire de Météorologie Physique (LaMP), CNRS/Université Blaise Pascal,
18 Clermont-Ferrand, France}

19 [7]{School of Physics and Centre for Climate & Air Pollution Studies, Ryan Institute,
20 National University of Ireland Galway, University Road, Galway, Ireland}

21

22

23 Correspondence to: S. Aksoyoglu (sebnem.aksoyoglu@psi.ch)

24 **Abstract**

25 We evaluated a modified VBS (Volatility Basis Set) scheme to treat biomass burning-like
26 organic aerosol (BBOA) implemented in CAMx (Comprehensive Air Quality Model with
27 extensions). The updated scheme was parameterized with novel wood combustion smog
28 chamber experiments using a hybrid VBS framework that accounts for a mixture of wood



29 burning organic aerosol precursors and their further functionalization and fragmentation in the
30 atmosphere. The new scheme was evaluated for one of the winter EMEP intensive campaigns
31 (February-March 2009) against aerosol mass spectrometer (AMS) measurements performed
32 at 11 sites in Europe. We found a considerable improvement for the modelled organic aerosol
33 (OA) mass compared to our previous model application with the mean fractional bias (MFB)
34 reduced from -61% to -29%.

35 We performed model-based source apportionment studies and compared results against
36 positive matrix factorization (PMF) analysis performed on OA AMS data. Both model and
37 observations suggest that OA was mainly of secondary origin at almost all sites. Modelled
38 secondary organic aerosol (SOA) contributions to total OA varied from 32 to 88% (with an
39 average contribution of 62%) and absolute concentrations were generally under-predicted.
40 Modelled primary hydrocarbon-like organic aerosol (HOA) and primary biomass burning-like
41 aerosol (BBOA) fractions contributed to a lesser extent (HOA from 3 to 30%, and BBOA
42 from 1 to 39%) with average contributions of 13 and 25%, respectively. Modelled BBOA
43 fractions was found to represent 12 to 64% of the total residential heating related OA, with
44 increasing contributions at stations located in the northern part of the domain.

45 Source apportionment studies were performed to assess the contribution of residential and
46 non-residential combustion precursors to the total SOA. Non-residential combustion and
47 transportation precursors contributed about 30-40% to SOA formation (with increasing
48 contributions at urban and near industrialized sites) whereas residential combustion (mainly
49 related to wood burning) contributed to a larger extent, around 60-70%. Contributions to OA
50 from residential combustion precursors in different volatility ranges were also assessed: our
51 results indicate that residential combustion gas-phase precursors in the semi-volatile range
52 contributed from 6 to 30%, with higher contributions predicted at stations located in the
53 southern part of the domain. On the other hand, higher volatility residential combustion
54 precursors contributed from 15 to 38% with no specific gradient among the stations.

55 The new retrieved parameterization, although leading to a better agreement between model
56 and observations, still under-predicts the SOA fraction suggesting remaining uncertainties in
57 the new scheme or that other sources and/or formation mechanisms need to be elucidated.

58



59 1 Introduction

60 Organic aerosol (OA) comprises the main fraction of fine particulate matter (PM_{10}) (Jimenez et
61 al., 2009). Even though the sources of its primary fraction (primary organic aerosol, POA) are
62 qualitatively known, uncertainties remain in terms of the total emission fluxes annually
63 released into the troposphere (Kuenen et al., 2014). Moreover, the measured OA load largely
64 exceeds the emitted POA fractions at most measurement sites around the world. A secondary
65 fraction (SOA), formed from the condensation of oxidized gases with low-volatility on pre-
66 existing particles, is found to be the dominant fraction of OA (Crippa et al., 2014; Huang et
67 al., 2014; Jimenez et al., 2009). Such low-volatility products are produced in the atmosphere
68 when higher volatility organic gases are oxidized by ozone (O_3), hydroxyl (OH) radical and/or
69 nitrate (NO_3) radical. The physical and chemical processes leading to the formation of SOA
70 are numerous, very uncertain and currently under debate (Hallquist et al., 2009; Tsigaridis et
71 al., 2014; Fuzzi et al., 2015; Woody et al., 2016).

72 Available long-term measurements might help in elucidating the composition and origin of
73 OA in different seasons. Canonaco et al. (2015) presented direct evidence for significant
74 changes in the SOA fingerprint between summer and winter from 13 months of OA
75 measurements conducted in Zürich using the aerosol chemical speciation monitor (ACSM).
76 Their results indicate that summer oxygenated OA mainly arises from biogenic precursors
77 whereas winter oxygenated OA is more strongly influenced by wood burning emissions.
78 Moreover, numerous ambient studies of open burning plumes from aircraft do not show a net
79 increase in OA, despite observing oxidation (Cubison et al., 2011; Jolleys et al., 2012). It is
80 therefore necessary that the chemical transport models (CTMs) correctly reproduce OA
81 concentrations by taking into account all the uncertainties and variability of observations.

82 Most of the CTMs account for common biogenic and anthropogenic high volatility SOA
83 precursors such as terpenes, isoprene, xylene and toluene which have a saturation
84 concentration (C^*) higher than $10^6 \mu\text{g m}^{-3}$ (Aksoyoglu et al., 2011; Ciarelli et al., 2016a). A
85 few models also include intermediate volatility organic compounds (IVOCs) with a C^* of 10^3
86 - $10^6 \mu\text{g m}^{-3}$ and semi-volatile organic compounds (SVOCs) with a C^* of 0.1 - $10^3 \mu\text{g m}^{-3}$ co-
87 emitted with POA (Bergström et al., 2012; Ciarelli et al., 2016a; Denier van der Gon et al.,
88 2015; Fountoukis et al., 2014; Tsimpidi et al., 2010; Woody et al., 2016). In these
89 applications, the volatility distributions of POA and IVOCs emissions are based on the study



90 of Robinson et al. (2007), where the IVOC mass is assumed to be 1.5 times the total organic
91 mass available in the semi-volatile range.

92 The standard gridded emission inventories do not yet include SVOCs and their emissions are
93 still highly uncertain as their measurement is strongly affected by the method used (Lipsky
94 and Robinson, 2006). A recent study by Denier van der Gon et al. (2015) reported a new
95 residential wood burning emission inventory including SVOCs, where emissions are higher
96 by a factor of 2-3 on average than those in the EUCAARI inventory (Kulmala et al., 2011).
97 The new emission inventory was used in two CTMs (EMEP and PMCAMx) and it improved
98 the model performance for the total OA (Denier van der Gon et al., 2015). Ciarelli et al.
99 (2016a) showed that allowing for evaporation of primary organic particles as available in
100 European emission inventories degraded OA performance (further under-predicted OA but
101 with POA and SOA components in a better agreement) whereas model performance improved
102 when volatility distributions that implicitly account for missing semi-volatile material
103 (increasing POA emissions by a factor of 3) were deployed.

104 Various modelling studies were performed by increasing POA emissions by a factor of 3 to
105 compensate for the missing gaseous emissions based on partitioning theory predictions
106 (Ciarelli et al., 2016a; Fountoukis et al., 2014; Shrivastava et al., 2011; Tsimpidi et al., 2010).
107 Fig. S1 shows the partitioning of $\sim 1 \mu\text{g m}^{-3}$ of POA at different temperatures using the latest
108 available volatility distribution for biomass burning (May et al., 2013). The ratio between the
109 available gas and particle phase material in the semi-volatile range is predicted to be roughly
110 3. This implies that, in these applications, the newly emitted organic mass (POA + SVOCs +
111 IVOCs) is 7.5 times higher than in original emissions (i.e., $\text{OM} = (3*\text{POA}) + (1.5*(3*\text{POA}))$).
112 This indirect accounting of missing organic material could be used in the absence of more
113 detailed gridded emission inventories, keeping in mind that the amount of higher volatility
114 compounds was specifically derived from studies conducted with diesel engines (Robinson et
115 al., 2007).

116 Along with ambient measurement studies, novel wood burning smog chamber studies provide
117 more insight into wood burning SOA formation and the nature of its precursors. Bruns et al.
118 (2016) performed several wood-burning aging experiments in a $\sim 7 \text{ m}^3$ smog chamber. Using
119 proton-transfer-reaction mass spectrometry (PTR-MS) they characterized SOA precursors at
120 the beginning of each aging experiment and found that up to 80% of the observed SOA could
121 be explained with a collection of a few SOA precursors that are usually not accounted in



122 regional CTMs (e.g. cresol, phenol, naphthalene). Recently, we used those chamber data to
123 parameterize a hybrid volatility basis set (Ciarelli et al., 2016b). The results provided new
124 direct information regarding the amount of wood burning SOA precursors which could be
125 directly used in CTM applications in the absence of more refined wood burning emissions in
126 gridded inventories. The box-model application reproduced the chamber data with an error of
127 approximately 25% on the OA mass and 15% on the O:C ratio (Ciarelli et al., 2016b).

128 In the current study, the updated volatility basis set (VBS) parameterization was implemented
129 in the comprehensive air quality model with extensions (CAMx) model, and simulations were
130 performed in Europe for a winter period in February-March 2009. Results are compared with
131 previous simulations using the original VBS framework (Ciarelli et al., 2016a) and with
132 source apportionment data at eleven sites with different exposure characteristics, obtained
133 using PMF applied to AMS measurements (Crippa et al., 2014).

134 **2 Method**

135 **2.1 Regional modelling with CAMx**

136 The CAMx version 5.41 with VBS scheme (ENVIRON, 2011; Koo et al., 2014) was used in this
137 study to simulate an EMEP measurement campaign between 25 February and 26 March 2009
138 in Europe. The modelling method and input data were the same as those used in the
139 EURODELTA III (ED III) project, described in detail in Ciarelli et al. (2016a). The model
140 domain covers Europe with a horizontal resolution of $0.25^\circ \times 0.25^\circ$. Meteorological
141 parameters were calculated from ECMWF IFS (Integrated Forecast System) data at 0.2°
142 resolution. There were 33 terrain-following σ -levels from ~ 20 m above ground level (first
143 layer) up to about 350 hPa, as in the original IFS data. For the gas phase chemistry, the
144 Carbon Bond (CB05) mechanism (Yarwood, 2005). The ISORROPIA thermodynamic model
145 (Nenes et al., 1998) was used for the partitioning of inorganic aerosols (sulfate, nitrate,
146 ammonium, sodium and chloride). Aqueous sulfate and nitrate formation in cloud water was
147 calculated using the RADM algorithm (Chang et al., 1987). Formation and evolution of OA is
148 treated with a hybrid volatility basis set (VBS) that accounts for changes in volatility and O:C
149 ratio (Koo et al., 2014) with dilution and aging. Particle size distributions were treated with a
150 two static mode scheme (fine and coarse). The results presented in this study refer to the fine
151 fraction ($PM_{2.5}$). We parameterized the biomass burning sets based on chamber data as
152 described in Ciarelli et al. (2016b).



153 The anthropogenic emission inventory was made available for the ED III community team by
154 the National Institute for Industrial Environment and Risks (INERIS) at $0.25^\circ \times 0.25^\circ$
155 horizontal resolution. More information regarding the anthropogenic emission inventories are
156 available in Bessagnet et al. (2014, 2016) and Ciarelli et al. (2016a). Hourly emissions of
157 biogenic VOCs, such as monoterpenes, isoprene, sesquiterpenes, xylene and toluene, were
158 calculated using the Model of Emissions of Gases and Aerosols from Nature MEGANv2.1
159 (Guenther et al., 2012) for each grid cell in the model domain.

160 **2.2 Biomass burning organic aerosol scheme**

161 The biomass burning organic aerosol scheme was constrained using recently available wood
162 burning smog chamber data (Bruns et al., 2016) as described in Ciarelli et al. (2016b). The
163 model deploys three different basis sets (Donahue et al., 2011) to simulate the emissions of
164 organics from biomass burning and their evolution in the atmosphere. The first set allocates
165 fresh emissions into five volatility bins ranging with saturation concentrations between 10^{-1}
166 and $10^3 \mu\text{g m}^{-3}$ following the volatility distribution and enthalpy of vaporization proposed by
167 May et al. (2013). In order to include gas-phase organics in the semi-volatile range in the
168 absence of more detailed inventory data, we used the approach proposed by previous studies
169 (Shrivastava et al., 2011; Tsimpidi et al., 2010). The second set allocates oxidation products
170 from SVOCs after shifting the volatility by one order of magnitude. The third set allocates
171 oxidation products from traditional VOCs (xylene, toluene, isoprene, monoterpenes and
172 sesquiterpenes) and from non-traditional SOA precursors retrieved from chamber data (~ 4.75
173 times the amount of organic material in the semi-volatile range, Ciarelli et al., 2016b).
174 Primary and secondary semi-volatile compounds react with OH in the gas-phase with a rate
175 constant of $4 \times 10^{-11} \text{ cm}^3 \text{ molec}^{-1} \text{ s}^{-1}$ (Donahue et al., 2013), which decreases their saturation
176 concentration by one order of magnitude. No heterogeneous oxidation of organic particles or
177 oligomerization processes is included in the model. The new model parameterization
178 described in this study is referred to as VBS_BC_NEW throughout the paper to distinguish
179 from the previous base case called VBS_BC as given in Ciarelli et al. (2016a).

180 **2.3 Model evaluation**

181 The model results for the period between 25 February and 26 March 2009 were compared
182 with OA concentrations measured by AMS at 11 European sites. Modelled BBOA, HOA and
183 SOA concentrations were compared with multi-linear engine 2 (ME-2) analysis performed on



184 AMS data (Paatero, 1999) using source finder (SoFi) (Canonaco et al., 2013; Crippa et al.,
185 2014). Elevated sites such as Montseny and Puy de Dôme were also included in the analysis
186 and modelled concentrations for these two sites were extracted from higher layers in order to
187 minimize the artefacts due to topography in a terrain-following coordinate system. This was
188 not the case in our previous application, where model OA concentrations were extracted from
189 the surface layer (Ciarelli et al., 2016a). We assumed POA emissions from SNAP2 (emissions
190 from non-industrial combustion plants in the Selected Nomenclature for Air Pollution) and
191 SNAP10 (emissions from agriculture, about 6% of POA in SNAP2) to be representative of
192 biomass burning like emissions. OA emissions from all other SNAP categories, including
193 emissions from ships, were compared with HOA-resolved PMF factors. Whilst this could be a
194 reasonable assumption for HOA-like aerosol, it is probably not the case for BBOA-like
195 aerosol, as gridded emissions for SNAP2 also include other emission sources (i.e., coal
196 burning which might be important in eastern European countries like Poland). We could not
197 resolve our emission inventory to that level and the contribution of coal could not be
198 separated for these European sites (Crippa et al., 2014) in contrast to China (Elser et al., 2016)
199 using similar statistical methods. Finally, the SOA fraction was compared to the PMF-
200 resolved oxygenated organic aerosol (OOA) fraction.

201 Statistics were reported in terms of mean bias (MB), mean error (ME), mean fractional bias
202 (MFB), mean fractional error (MFE) and coefficient of determination (R^2) (see Table S1 for
203 the definition of statistical parameters).

204 **3 Results and discussions**

205 **3.1 Analysis of the modelled OA**

206 Figure 1 shows the average modelled OA concentrations and surface temperature for the
207 period between 25 February and 26 March 2009. Temperatures were below 0°C in the north,
208 ranged 5-10°C in central Europe and were above 10°C in the southern part of the domain.
209 Model performance for surface temperature was evaluated within the ED III exercise and
210 found to be reproduced reasonably well, with a general under-prediction of around 1°C
211 (Bessagnet et al., 2014).

212 A clear spatial variability in the modelled OA concentrations is observed (Fig. 1). Predicted
213 OA concentrations were higher in eastern European countries (especially Romania and
214 southern Poland) as well as over northern Italy (8-10 $\mu\text{g m}^{-3}$ on average) whereas they were



215 lower in the northern part of the domain. A similar spatial distribution of OA concentrations
216 was also reported by Denier van der Gon et al. (2015) using the EMEP model. Relatively high
217 OA concentrations over the Mediterranean Sea are mainly of secondary origin due to
218 enhanced photochemical activity (more details are found in Section 3.2). In addition, the
219 reduced deposition capacity over water leads to higher OA levels.

220 The scatter plots in Fig. 2 show the modelled (VBS_BC_NEW) versus measured daily
221 average OA concentrations at 11 sites in Europe together with the results from our previous
222 model application (VBS_BC, Ciarelli et al., 2016a) for comparison. The modified VBS
223 scheme (VBS_BC_NEW) predicts higher OA concentrations compared to our previous study
224 using the original scheme (VBS_BC) (~ 60% more OA on average at all sites). Statistical
225 parameters improved significantly (Table 1); the mean fractional bias MFB decreased from -
226 61% in VBS_BC to -29% in VBS_BC_NEW and the model performance criteria were met
227 (Boylan and Russell, 2006). The coefficient of determination remained almost unchanged for
228 OA in the VBS_BC_NEW case ($R^2=0.58$) compared to VBS_BC ($R^2=0.57$) indicating that the
229 original model was able to similarly capture the OA daily variation, but not its magnitude.
230 The majority of the stations show an $R^2 \geq 0.4$. Lower values were found for the elevated sites
231 of Montseny and Puy de Dome ($R^2=0.17$ and $R^2=0.13$, respectively) and also at the Helsinki
232 site ($R^2=0.06$). In spite of the improvements with respect to earlier studies, modelled OA is
233 still lower than measured (mean bias MB from $-0.1 \mu\text{g m}^{-3}$ up to $-3.1 \mu\text{g m}^{-3}$) at most of the
234 sites, with only a slight overestimation at a few locations (MB from $0.3 \mu\text{g m}^{-3}$ up to $0.9 \mu\text{g m}^{-3}$).
235

236 The observed OA gradient among the 11 sites was reproduced very well (Fig. 3). Both
237 measured and modelled OA concentrations were highest in Barcelona. Other sites with
238 concentrations greater than $2 \mu\text{g m}^{-3}$ were Payerne, Helsinki, Vavihill and Montseny.
239 Barcelona and Helsinki are both classified as urban stations, which justifies the higher OA
240 loads due to the anthropogenic activities (e.g. traffic, cooking and heating). Anthropogenic
241 activities in the area of Barcelona could also affect OA concentrations at Montseny which is
242 about 40 km away. In the case of Payerne and Vavihill, the relatively high OA concentrations
243 might be due to residential heating, where wood is largely used as a combustion fuel during
244 cold periods (Denier van der Gon et al., 2015). For Chilbolton, located not far from London,
245 this might not be the case: the fuel wood usage in the UK is the lowest in Europe (Denier van
246 der Gon et al., 2015). Ots et al. (2016) suggested the possibility of missing diesel-related



247 IVOCs emissions, which might be an important source of SOA in those regions. However,
248 other studies reported substantial contribution from solid fuel combustion to OA (Young et
249 al., 2015). In this case, it might be that difficulties in reproducing the OA concentration are
250 mainly related to the relatively complex area of the site (i.e., close to the English Channel).
251 An evaluation of diurnal variations of HOA and SOA concentrations for this site showed a
252 consistent under-prediction of both components (Fig. S2).

253 3.2 Analysis of the OA components

254 The predicted POA spatial distribution (Fig. 4) resembles the residential heating emission
255 pattern of different countries (Bergström et al., 2012). The highest POA concentrations were
256 predicted in east European countries, France, Portugal and in northern Italy ($\sim 3\text{-}5 \mu\text{g m}^{-3}$)
257 whereas they were less than $1 \mu\text{g m}^{-3}$ in the rest of the model domain. Very low OA
258 concentrations in Sweden were already shown by previous European studies. Bergström et al.
259 (2012) reported that Swedish organic carbon (OC) emissions from the residential heating
260 sector were lower by a factor of 14 compared to Norway, even though Sweden had much
261 higher wood usage (60% higher) likely due to underestimation of emissions from residential
262 heating in the emission inventory.

263 The spatial distribution of SOA concentrations, on the other hand, is more widespread with a
264 visible north to south gradient (Fig. 4). Higher SOA concentration were predicted close to
265 primary emission sources (e.g. Poland, Romania, Po Valley and Portugal) but also in most of
266 the countries below 50° latitude and over the Mediterranean Sea where higher OH
267 concentration, reduced deposition capacity and high contribution from long-range transport
268 are expected (average concentrations around $3\text{-}4 \mu\text{g m}^{-3}$).

269 Comparison of results from this study (VBS_BC_NEW) with the earlier one (VBS_BC,
270 Ciarelli et al., 2016a) suggests that the new VBS scheme predicts higher SOA concentrations
271 by about a factor of 3 (Fig. 5) and improves the model performance when comparing assessed
272 OOA from measurements with modelled SOA (Table 3).

273 POA concentrations, on the other hand, are clustered below $1 \mu\text{g m}^{-3}$ except in Barcelona,
274 showing an $R^2=0.36$, (Fig. 5 and Table 2). Although predicted POA concentrations at
275 Barcelona were lower than the measurements, MFB=-47% and MFE=69% were still in the
276 range for acceptable performance criteria ($MFE \leq +75\%$ and $-60 < MFB < +60\%$, Boylan
277 and Russell, 2006). On the other hand, the model over-predicted the POA concentrations at



278 Hyytiälä (MFB=131% and MFE=131%), Helsinki (MFB=95% and MFE=100%) and Cabauw
279 (MFB=76% and MFE=86%) mainly due to the overestimated BBOA fraction as seen in Fig.
280 6.

281 At most of the sites, OA was dominated by SOA (Fig. 6 and Fig. 7) which was
282 underestimated in particular at Chilbolton, Melpitz and Vavihill (Table 3). As already
283 mentioned, the under-prediction of SOA concentrations might be attributed to missing SOA
284 precursors or uncertainties in SOA formation mechanisms and removal processes. On the
285 other hand, the remote station of Mace Head showed a positive bias for SOA (MFB = 30%),
286 even though model and measurement concentrations were very similar (0.54 and $0.35 \mu\text{g m}^{-3}$,
287 respectively), which could be attributed to an overestimated contribution from the boundaries.
288 The relatively small positive bias at the two elevated sites, Montseny and Puy de Dome (MFB
289 = 4% and 17%, respectively), is most likely the result of difficulties in capturing the inversion
290 layer.

291 Mostly traffic-related HOA was underestimated at the urban site Barcelona (Table S2, Fig. 6),
292 with the model not able to reproduce the diurnal variation of HOA at this urban site likely due
293 to poorly reproduced meteorological conditions or too much dilution during day time in the
294 model (Fig. S2). The under-prediction of the HOA fraction is consistent with our previous
295 study where model evaluation for NO_2 revealed a systematic under-estimation of the
296 modelled concentration (Ciarelli et al., 2016a). The course resolution of the domain ($0.25^\circ \times$
297 0.25°) may result in too low emissions especially at urban sites. The majority of the NO_x
298 ($\text{NO}+\text{NO}_2$) emissions in Europe arises from the transportation sector (SNAP7), which might
299 have much larger uncertainties than previously thought (Vaughan et al., 2016). An evaluation
300 of planetary boundary layer height (PBLH) within the EDIII shows that although the PBLH
301 was quite well represented in general in the ECMWF IFS meteorological fields, CAMx tends
302 to underestimate the night-time minima and to overestimate some daytime peaks. The other
303 urban site considered in this study is Helsinki. In this case, HOA concentrations were over-
304 predicted, as seen in Figs. 6 and S2, which might indicate missing dispersion processes in the
305 model or under-estimated dilution.

306 The modelled BBOA fraction on the other hand was generally higher than the measurements,
307 with an average MFB of 50% (Table S3, Figs. 6-7), which might arise from various factors:
308 1) In the model, POA emissions from SNAP2 and SNAP10 are assumed to be representative
309 of BBOA emissions which might not be the case for all European countries (other non-wood



310 fuels such as coal, which is allocated to SNAP2 category and could not be separated in this
311 study), 2) The under-prediction of the modelled surface temperature (Bessagnet et al., 2014)
312 will directly influence the partitioning of organic material in the semi-volatile range,
313 favouring freshly emitted organic material to condense more to the particle phase, 3)
314 Uncertainties in the adopted volatility distributions and/or in the oxidation processes of semi-
315 volatile organic vapours.

316 The temporal variability of OA concentrations was reproduced quite well: most of the peaks
317 were captured accurately (Fig. 8); the magnitudes of only a few (Vavihill, Chilbolton and
318 Barcelona) were underestimated. Diurnal variations of HOA, BBOA and SOA components at
319 the rural-background sites suggest that the model was able to reproduce the relatively flat
320 profile of the measured SOA and the increased BBOA concentrations at night (Fig. 9). On the
321 other hand, there was a slight underestimation of HOA during the day, especially around
322 noon, likely as a result of too much dilution in the model.

323 In our previous application, we performed a sensitivity study with increased biogenic and
324 residential heating emissions by a factor of two (Ciarelli et al., 2016a). While the model was
325 rather insensitive to the increased biogenic emissions during winter periods, a substantial
326 increase in the OA concentrations was observed when emissions from residential heating
327 were doubled. The model with doubled emissions from residential heating
328 (VBC_BC_2xBBOA), overestimated the POA fraction at most of the sites (Fig. 10) with
329 smaller effects on SOA, even though a better closure was achieved between modelled and
330 observed OA. The results of the simulations using the new parameterization
331 (VBC_BC_NEW), on the other hand, were closer to the measurement data especially for the
332 SOA fraction (Fig. 10).

333 3.3 Residential versus non-residential combustion precursors

334 More detailed source apportionment studies were performed in order to assess the importance
335 of residential and non-residential combustion precursors for OA and SOA. The upper panel in
336 Fig. 11 shows the relative contributions to SOA from residential and non-residential
337 combustion precursors. The model results indicate that non-residential combustion and
338 transportation precursors contribute about 30-40% to SOA formation (with increasing
339 contribution at urban and near-industrialized sites) whereas residential combustion (mainly
340 related to wood burning) contribute to a larger extent, i.e., around 60-70%. The residential



341 combustion precursors were further apportioned to semi-volatile and higher volatility
342 precursors (Fig. 11, lower panel). In particular, SVOC precursors exhibit a south-to-north
343 gradient with increasing contribution to the residential heating related OA for stations located
344 in the southern part of the domain (maximum and minimum contributions of 42 and 17% in
345 Montseny and Hyytiälä, respectively). Such a gradient also reflects the effect of temperature
346 on the partitioning of semi-volatile organic material: the lower temperatures in the northern
347 part of the domain will reduce the saturation concentration of the organic compounds
348 allowing primary organic material to favour the particle phase and reducing the amount of
349 SVOCs available that could act as SOA precursors. In the southern part of the domain, the
350 higher temperature will favour more organic material in the semi-volatile range to reside in
351 the gas-phase, rendering it available for oxidation. On the other hand, no south-to-north
352 gradient was predicted for the higher volatility class of precursors. Source apportionment for
353 different volatilities classes of the non-residential and transportation sectors is currently not
354 implemented for this model application.

355 A comprehensive summary of the contribution to the total OA from all the sources (i.e. HOA,
356 BBOA, residential combustion semi-volatile precursors, residential combustion higher
357 volatility precursors and non-residential combustion precursors) is shown in Fig. 12 at each of
358 the measurement sites. Residential combustion precursors in the semi-volatile range
359 contributed from 6 to 30% whereas higher volatility compounds contributed to a larger extent,
360 i.e. from 15 to 38%. SOA from non-residential combustion precursors contributed from 10 to
361 37% to the total OA. The primary sources HOA and BBOA contributed from 3 to 30% and 1-
362 39%, respectively. These results lead to the conclusion that the overall contribution of
363 residential combustion to OA concentrations in Europe varies between 52% at stations in the
364 UK and 75-76% at stations in Scandinavia.

365 **Conclusion**

366 This study aims to evaluate recent VBS parameterizations in commonly used CTMs and to
367 underline the importance of taking into account updated and more detailed SOA schemes as
368 new ambient and chamber measurements elucidate the high complexity and strong variability
369 of OA. In this context, a new VBS parameterization (based on recent wood burning
370 experiments) implemented in CAMx was evaluated against high-resolution AMS
371 measurements at 11 sites in Europe during February-March 2009, one of the winter EMEP
372 intensive measurement campaigns. Results obtained from this study were compared with



373 those from our earlier work in which the original VBS scheme in CAMx was applied. A
374 detailed source apportionment for the organic aerosol (OA) fraction was discussed. This study
375 provided the following outcome:

376 - A considerable improvement was found for the modelled OA concentrations
377 compared to our previous studies mainly due to the improved secondary organic
378 aerosol (SOA) performance. The average bias for the 11 AMS sites decreased by
379 about 60% although the model still underestimates the SOA fraction.

380 - Both model and PMF source apportionment based on measurements suggested that
381 OA was mainly of secondary origin with smaller primary contribution, with primary
382 contribution of 13 and 25% for HOA and BBOA, respectively. The model
383 performance for the HOA fraction was reasonably good at most of the sites except at
384 the urban Barcelona site which could be related to the uncertainties in emissions or too
385 much dilution in the model. On the other hand, the modelled BBOA was higher than
386 the measurements at several stations indicating the need for further studies on
387 residential heating emissions, their volatility distribution and oxidation pathway of the
388 semi-volatile organic gases.

389 - Emissions from the residential heating sector (SNAP2) largely influenced the OA
390 composition. The modeled primary BBOA fraction contributed from 46% to 77% of
391 the total primary organic fraction (POA), with an average contribution of 65%. Non-
392 residential combustion and transportation precursors contributed about 30-40% to
393 SOA (with increasing contribution at urban and near-industrialized sites) whereas
394 residential combustion (mainly related to wood burning) contributes to a larger extent,
395 ~ 60-70%. Moreover, the contribution to OA from residential combustion precursors
396 in different range of volatilities was also investigated: residential combustion gas-
397 phase precursors in the semi-volatile range contributed from 6 to 30% with a positive
398 south-to-north gradient. On the other hand, higher volatility residential combustion
399 precursors contributed from 15 to 38% showing no specific gradient among the
400 stations.

401



402 **Acknowledgements**

403 We thank the EURODELTA III modelling community, especially INERIS, TNO as well as
404 ECMWF for providing various model input data. Calculations of land use data were
405 performed at the Swiss National Supercomputing Centre (CSCS). We thank D. Oderbolz for
406 developing the CAMxRunner framework to ensure reproducibility and data quality among the
407 simulations and sensitivity tests. M. Tinguely for the visualization software, and RAMBOLL
408 ENVIRON for their valuable comments. This study was financially supported by the Swiss
409 Federal Office of Environment (FOEN). The research leading to these results received
410 funding from the European Community's Seventh Framework Programme (FP7/2007-2013)
411 under grant agreement no. 290605 (PSI-FELLOW), from the Competence Center
412 Environment and Sustainability (CCES) (project OPTIWARES) and from the Swiss National
413 Science Foundation (WOOSHI grant 140590). We thank D.A. Day for analysis on the
414 DAURE dataset. Erik Swietlicki for the Vavihill dataset, Claudia Mohr for the Barcelona
415 dataset, A. Kiendler-Scharr for Cabauw AMS data, Eriko Nemitz for the Chilboton data,
416 Karine Sellegri for the Puy de Dôme dataset and Jose-Luis Jimenez for the measurements data
417 in Montseny. The AMS measurements were funded through the European EUCAARI IP. We
418 would like to acknowledge EMEP for the measurement data used here, HEA-PRTL14, EPA
419 Ireland, and the Science Foundation Ireland for facilitating measurements at Mace Head.

420

421

422

423

424

425

426

427

428

429

430



431

432

433 **References**

434 Aksoyoglu, S., Keller, J., Barmpadimos, I., Oderbolz, D., Lanz, V. A., Prévôt, A. S. H. and
435 Baltensperger, U.: Aerosol modelling in Europe with a focus on Switzerland during summer
436 and winter episodes, *Atmos. Chem. Phys.*, 11(14), 7355–7373, doi:10.5194/acp-11-7355-
437 2011, 2011.

438 Bergström, R., Denier van der Gon, H. A. C., Prévôt, A. S. H., Yttri, K. E. and Simpson, D.:
439 Modelling of organic aerosols over Europe (2002–2007) using a volatility basis set (VBS)
440 framework: application of different assumptions regarding the formation of secondary organic
441 aerosol, *Atmos. Chem. Phys.*, 12(18), 8499–8527, doi:10.5194/acp-12-8499-2012, 2012.

442 Bessagnet, B., Colette, A., Meleux, F., Rouil, L., Ung, A., Favez, O., Cuvelier, C., Thunis, P.,
443 Tsyro, S., Stern, R., Manders, A., Kranenburg, R., Aulinger, A., Bieser, J., Mircea, M.,
444 Briganti, A., Cappelletti, A., Calori, G., Finardi, S., Silibello, C., Ciarelli, G., Aksoyoglu, S.,
445 Prévôt, A., Pay, M. T., Baldasano, J. M., García Vivanco, M., Garrido, J. L., Palomino, I.,
446 Martín, F., Pirovano, G., Roberts, P., Gonzalez, L., White, L., Menut, L., Dupont, J. C.,
447 Carnevale, C. and Pederzoli, A.: The EURODELTA III exercise – Model evaluation with
448 observations issued from the 2009 EMEP intensive period and standard measurements in
449 Feb/Mar 2009, 2014.

450 Boylan, J. W. and Russell, A. G.: PM and light extinction model performance metrics, goals,
451 and criteria for three-dimensional air quality models, *Atmos. Environ.*, 40(26), 4946–4959,
452 doi:10.1016/j.atmosenv.2005.09.087, 2006.

453 Bruns, E. A., El Haddad, I., Slowik, J. G., Kilic, D., Klein, F., Baltensperger, U. and Prévôt,
454 A. S. H.: Identification of significant precursor gases of secondary organic aerosols from
455 residential wood combustion, *Sci. Rep.*, 6, 27881, doi:10.1038/srep27881, 2016.

456 Canonaco, F., Crippa, M., Slowik, J. G., Baltensperger, U. and Prévôt, A. S. H.: SoFi, an
457 IGOR-based interface for the efficient use of the generalized multilinear engine (ME-2) for
458 the source apportionment: ME-2 application to aerosol mass spectrometer data, *Atmos. Meas.*
459 *Tech.*, 6(12), 3649–3661, doi:10.5194/amt-6-3649-2013, 2013.



- 460 Canonaco, F., Slowik, J. G., Baltensperger, U. and Prévôt, A. S. H.: Seasonal differences in
461 oxygenated organic aerosol composition: implications for emissions sources and factor
462 analysis, *Atmos. Chem. Phys.*, 15(12), 6993–7002, doi:10.5194/acp-15-6993-2015, 2015.
- 463 Chang, J. S., Brost, R. A., Isaksen, I. S. A., Madronich, S., Middleton, P., Stockwell, W. R.
464 and Walcek, C. J.: A three-dimensional Eulerian acid deposition model: Physical concepts
465 and formulation, *J. Geophys. Res. Atmospheres*, 92(D12), 14681–14700,
466 doi:10.1029/JD092iD12p14681, 1987.
- 467 Ciarelli, G., Aksoyoglu, S., Crippa, M., Jimenez, J.-L., Nemitz, E., Sellegri, K., Äijälä, M.,
468 Carbone, S., Mohr, C., O’Dowd, C., Poulain, L., Baltensperger, U. and Prévôt, A. S.
469 H.: Evaluation of European air quality modelled by CAMx including the volatility basis set
470 scheme, *Atmos. Chem. Phys.*, 16(16), 10313–10332, doi:10.5194/acp-16-10313-2016, 2016a.
- 471 Ciarelli, G., El Haddad, I., Bruns, E., Aksoyoglu, S., Möhler, O., Baltensperger, U. and
472 Prévôt, A. S. H.: Constraining a hybrid volatility basis set model for aging of wood burning
473 emissions using smog chamber experiments, *Geosci. Model Dev. Discuss.*, 1–31,
474 doi:10.5194/gmd-2016-163, 2016b.
- 475 Crippa, M., Canonaco, F., Lanz, V. A., Äijälä, M., Allan, J. D., Carbone, S., Capes, G.,
476 Ceburnis, D., Dall’Osto, M., Day, D. A., DeCarlo, P. F., Ehn, M., Eriksson, A., Freney, E.,
477 Hildebrandt Ruiz, L., Hillamo, R., Jimenez, J. L., Junninen, H., Kiendler-Scharr, A.,
478 Kortelainen, A.-M., Kulmala, M., Laaksonen, A., Mensah, A. A., Mohr, C., Nemitz, E.,
479 O’Dowd, C., Ovadnevaite, J., Pandis, S. N., Petäjä, T., Poulain, L., Saarikoski, S., Sellegri,
480 K., Swietlicki, E., Tiitta, P., Worsnop, D. R., Baltensperger, U. and Prévôt, A. S. H.: Organic
481 aerosol components derived from 25 AMS data sets across Europe using a consistent ME-2
482 based source apportionment approach, *Atmos. Chem. Phys.*, 14(12), 6159–6176,
483 doi:10.5194/acp-14-6159-2014, 2014.
- 484 Cubison, M. J., Ortega, A. M., Hayes, P. L., Farmer, D. K., Day, D., Lechner, M. J., Brune,
485 W. H., Apel, E., Diskin, G. S., Fisher, J. A., Fuelberg, H. E., Hecobian, A., Knapp, D. J.,
486 Mikoviny, T., Riemer, D., Sachse, G. W., Sessions, W., Weber, R. J., Weinheimer, A. J.,
487 Wisthaler, A. and Jimenez, J. L.: Effects of aging on organic aerosol from open biomass
488 burning smoke in aircraft and laboratory studies, *Atmos. Chem. Phys.*, 11(23), 12049–12064,
489 doi:10.5194/acp-11-12049-2011, 2011.



- 490 Denier van der Gon, H. A. C., Bergström, R., Fountoukis, C., Johansson, C., Pandis, S. N.,
491 Simpson, D. and Visschedijk, A. J. H.: Particulate emissions from residential wood
492 combustion in Europe – revised estimates and an evaluation, *Atmos. Chem. Phys.*, 15(11),
493 6503–6519, doi:10.5194/acp-15-6503-2015, 2015.
- 494 Donahue, N. M., Epstein, S. A., Pandis, S. N. and Robinson, A. L.: A two-dimensional
495 volatility basis set: 1. organic-aerosol mixing thermodynamics, *Atmos. Chem. Phys.*, 11(7),
496 3303–3318, doi:10.5194/acp-11-3303-2011, 2011.
- 497 Donahue, N. M., Chuang, W., Epstein, S. A., Kroll, J. H., Worsnop, D. R., Robinson, A. L.,
498 Adams, P. J. and Pandis, S. N.: Why do organic aerosols exist? Understanding aerosol
499 lifetimes using the two-dimensional volatility basis set, *Environ. Chem.*, 10(3), 151,
500 doi:10.1071/EN13022, 2013.
- 501 Elser, M., Huang, R.-J., Wolf, R., Slowik, J. G., Wang, Q., Canonaco, F., Li, G., Bozzetti, C.,
502 Daellenbach, K. R., Huang, Y., Zhang, R., Li, Z., Cao, J., Baltensperger, U., El-Haddad, I.
503 and Prévôt, A. S. H.: New insights into PM_{2.5} chemical composition and sources in two
504 major cities in China during extreme haze events using aerosol mass spectrometry, *Atmos.*
505 *Chem. Phys.*, 16(5), 3207–3225, doi:10.5194/acp-16-3207-2016, 2016.
- 506 ENVIRON: User's Guide, Comprehensive Air Quality Model with Extensions (CAMx),
507 Version 5.40, Environ International Corporation, California, 2011.
- 508 Fountoukis, C., Megaritis, A. G., Skyllakou, K., Charalampidis, P. E., Pilinis, C., Denier van
509 der Gon, H. A. C., Crippa, M., Canonaco, F., Mohr, C., Prévôt, A. S. H., Allan, J. D., Poulain,
510 L., Petäjä, T., Tiitta, P., Carbone, S., Kiendler-Scharr, A., Nemitz, E., O'Dowd, C., Swietlicki,
511 E. and Pandis, S. N.: Organic aerosol concentration and composition over Europe: insights
512 from comparison of regional model predictions with aerosol mass spectrometer factor
513 analysis, *Atmos. Chem. Phys.*, 14(17), 9061–9076, doi:10.5194/acp-14-9061-2014, 2014.
- 514 Grieshop, A. P., Logue, J. M., Donahue, N. M. and Robinson, A. L.: Laboratory investigation
515 of photochemical oxidation of organic aerosol from wood fires 1: measurement and
516 simulation of organic aerosol evolution, *Atmos. Chem. Phys.*, 9(4), 1263–1277,
517 doi:10.5194/acp-9-1263-2009, 2009.
- 518 Guenther, A. B., Jiang, X., Heald, C. L., Sakulyanontvittaya, T., Duhl, T., Emmons, L. K. and
519 Wang, X.: The Model of Emissions of Gases and Aerosols from Nature version 2.1



- 520 (MEGAN2.1): an extended and updated framework for modeling biogenic emissions, *Geosci.*
521 *Model Dev.*, 5(6), 1471–1492, doi:10.5194/gmd-5-1471-2012, 2012.
- 522 Hallquist, M., Wenger, J. C., Baltensperger, U., Rudich, Y., Simpson, D., Claeys, M.,
523 Dommen, J., Donahue, N. M., George, C., Goldstein, A. H., Hamilton, J. F., Herrmann, H.,
524 Hoffmann, T., Iinuma, Y., Jang, M., Jenkin, M. E., Jimenez, J. L., Kiendler-Scharr, A.,
525 Maenhaut, W., McFiggans, G., Mentel, T. F., Monod, A., Prévôt, A. S. H., Seinfeld, J. H.,
526 Surratt, J. D., Szmigielski, R. and Wildt, J.: The formation, properties and impact of
527 secondary organic aerosol: current and emerging issues, *Atmos. Chem. Phys.*, 9(14), 5155–
528 5236, doi:10.5194/acp-9-5155-2009, 2009.
- 529 Huang, R.-J., Zhang, Y., Bozzetti, C., Ho, K.-F., Cao, J.-J., Han, Y., Daellenbach, K. R.,
530 Slowik, J. G., Platt, S. M., Canonaco, F., Zotter, P., Wolf, R., Pieber, S. M., Brun, E. A.,
531 Crippa, M., Ciarelli, G., Piazzalunga, A., Schwikowski, M., Abbaszade, G., Schnelle-Kreis,
532 J., Zimmermann, R., An, Z., Szidat, S., Baltensperger, U., Haddad, I. E. and Prévôt, A. S. H.:
533 High secondary aerosol contribution to particulate pollution during haze events in China,
534 *Nature*, 514(7521), 218–222, doi:10.1038/nature13774, 2014.
- 535 Jimenez, J. L., Canagaratna, M. R., Donahue, N. M., Prevot, A. S. H., Zhang, Q., Kroll, J. H.,
536 DeCarlo, P. F., Allan, J. D., Coe, H., Ng, N. L., Aiken, A. C., Docherty, K. S., Ulbrich, I. M.,
537 Grieshop, A. P., Robinson, A. L., Duplissy, J., Smith, J. D., Wilson, K. R., Lanz, V. A.,
538 Hueglin, C., Sun, Y. L., Tian, J., Laaksonen, A., Raatikainen, T., Rautiainen, J., Vaattovaara,
539 P., Ehn, M., Kulmala, M., Tomlinson, J. M., Collins, D. R., Cubison, M. J., Dunlea, E. J.,
540 Huffman, J. A., Onasch, T. B., Alfarra, M. R., Williams, P. I., Bower, K., Kondo, Y.,
541 Schneider, J., Drewnick, F., Borrmann, S., Weimer, S., Demerjian, K., Salcedo, D., Cottrell,
542 L., Griffin, R., Takami, A., Miyoshi, T., Hatakeyama, S., Shimojo, A., Sun, J. Y., Zhang, Y.
543 M., Dzepina, K., Kimmel, J. R., Sueper, D., Jayne, J. T., Herndon, S. C., Trimborn, A. M.,
544 Williams, L. R., Wood, E. C., Middlebrook, A. M., Kolb, C. E., Baltensperger, U. and
545 Worsnop, D. R.: Evolution of organic aerosols in the atmosphere, *Science*, 326(5959), 1525–
546 1529, doi:10.1126/science.1180353, 2009.
- 547 Jolleys, M. D., Coe, H., McFiggans, G., Capes, G., Allan, J. D., Crosier, J., Williams, P. I.,
548 Allen, G., Bower, K. N., Jimenez, J. L., Russell, L. M., Grutter, M. and Baumgardner, D.:
549 Characterizing the Aging of Biomass Burning Organic Aerosol by Use of Mixing Ratios: A
550 Meta-analysis of Four Regions, *Environ. Sci. Technol.*, 46(24), 13093–13102,
551 doi:10.1021/es302386v, 2012.



- 552 Koo, B., Knipping, E. and Yarwood, G.: 1.5-Dimensional volatility basis set approach for
553 modeling organic aerosol in CAMx and CMAQ, *Atmos. Environ.*, 95, 158–164,
554 doi:10.1016/j.atmosenv.2014.06.031, 2014.
- 555 Kuenen, J. J. P., Visschedijk, A. J. H., Jozwicka, M. and Denier van der Gon, H. A. C.: TNO-
556 MACC-II emission inventory; a multi-year (2003–2009) consistent high-resolution European
557 emission inventory for air quality modelling, *Atmos. Chem. Phys.*, 14(20), 10963–10976,
558 doi:10.5194/acp-14-10963-2014, 2014.
- 559 Kulmala, M., Asmi, A., Lappalainen, H. K., Baltensperger, U., Brenguier, J.-L., Facchini, M.
560 C., Hansson, H.-C., Hov, Ø., O’Dowd, C. D., Pöschl, U., Wiedensohler, A., Boers, R.,
561 Boucher, O., de Leeuw, G., Denier van der Gon, H. A. C., Feichter, J., Krejci, R., Laj, P.,
562 Lihavainen, H., Lohmann, U., McFiggans, G., Mentel, T., Pilinis, C., Riipinen, I., Schulz, M.,
563 Stohl, A., Swietlicki, E., Vignati, E., Alves, C., Amann, M., Ammann, M., Arabas, S., Artaxo,
564 P., Baars, H., Beddows, D. C. S., Bergström, R., Beukes, J. P., Bilde, M., Burkhardt, J. F.,
565 Canonaco, F., Clegg, S. L., Coe, H., Crumeyrolle, S., D’Anna, B., Decesari, S., Gilardoni, S.,
566 Fischer, M., Fjaeraa, A. M., Fountoukis, C., George, C., Gomes, L., Halloran, P., Hamburger,
567 T., Harrison, R. M., Herrmann, H., Hoffmann, T., Hoose, C., Hu, M., Hyvärinen, A., Hörrak,
568 U., Iinuma, Y., Iversen, T., Josipovic, M., Kanakidou, M., Kiendler-Scharr, A., Kirkevåg, A.,
569 Kiss, G., Klimont, Z., Kolmonen, P., Komppula, M., Kristjánsson, J.-E., Laakso, L.,
570 Laaksonen, A., Labonnote, L., Lanz, V. A., Lehtinen, K. E. J., Rizzo, L. V., Makkonen, R.,
571 Manninen, H. E., McMeeking, G., Merikanto, J., Minikin, A., Mirme, S., Morgan, W. T.,
572 Nemitz, E., O’Donnell, D., Panwar, T. S., Pawlowska, H., Petzold, A., Pienaar, J. J., Pio, C.,
573 Plass-Duelmer, C., Prévôt, A. S. H., Pryor, S., Reddington, C. L., Roberts, G., Rosenfeld, D.,
574 Schwarz, J., Seland, Ø., et al.: General overview: European Integrated project on Aerosol
575 Cloud Climate and Air Quality interactions (EUCAARI) – integrating aerosol research from
576 nano to global scales, *Atmos. Chem. Phys.*, 11, 13061–13143, doi:10.5194/acp-11-13061-
577 2011, 2011.
- 578 Lipsky, E. M. and Robinson, A. L.: Effects of Dilution on Fine Particle Mass and Partitioning
579 of Semivolatile Organics in Diesel Exhaust and Wood Smoke, *Environ. Sci. Technol.*, 40(1),
580 155–162, doi:10.1021/es050319p, 2006.
- 581 May, A. A., Levin, E. J. T., Hennigan, C. J., Riipinen, I., Lee, T., Collett, J. L., Jimenez, J. L.,
582 Kreidenweis, S. M. and Robinson, A. L.: Gas-particle partitioning of primary organic aerosol



- 583 emissions: 3. Biomass burning, *J. Geophys. Res. Atmospheres*, 118(19), 2013JD020286,
584 doi:10.1002/jgrd.50828, 2013.
- 585 Nenes, A., Pandis, S. N. and Pilinis, C.: ISORROPIA: a new thermodynamic equilibrium
586 model for multiphase multicomponent inorganic aerosols, *Aquat. Geochem.*, 4, 123–152,
587 1998., *Aquat. Geochem.*, 4, 123–152, 1998.
- 588 Ots, R., Young, D. E., Vieno, M., Xu, L., Dunmore, R. E., Allan, J. D., Coe, H., Williams, L.
589 R., Herndon, S. C., Ng, N. L., Hamilton, J. F., Bergström, R., Di Marco, C., Nemitz, E.,
590 Mackenzie, I. A., Kuenen, J. J. P., Green, D. C., Reis, S. and Heal, M. R.: Simulating
591 secondary organic aerosol from missing diesel-related intermediate-volatility organic
592 compound emissions during the Clean Air for London (ClearLo) campaign, *Atmos. Chem.*
593 *Phys.*, 16(10), 6453–6473, doi:10.5194/acp-16-6453-2016, 2016.
- 594 Paatero, P.: The Multilinear Engine: A Table-Driven, Least Squares Program for Solving
595 Multilinear Problems, including the n-Way Parallel Factor Analysis Model, *J. Comput.*
596 *Graph. Stat.*, 8(4), 854, doi:10.2307/1390831, 1999.
- 597 Robinson, A. L., Donahue, N. M., Shrivastava, M. K., Weitkamp, E. A., Sage, A. M.,
598 Grieshop, A. P., Lane, T. E., Pierce, J. R. and Pandis, S. N.: Rethinking Organic Aerosols:
599 Semivolatile Emissions and Photochemical Aging, *Science*, 315(5816), 1259–1262,
600 doi:10.1126/science.1133061, 2007.
- 601 Shrivastava, M., Fast, J., Easter, R., Gustafson Jr., W. I., Zaveri, R. A., Jimenez, J. L., Saide,
602 P. and Hodzic, A.: Modeling organic aerosols in a megacity: comparison of simple and
603 complex representations of the volatility basis set approach, *Atmos. Chem. Phys.*, 11, 6639–
604 6662, 2011.
- 605 Tsigaridis, K., Daskalakis, N., Kanakidou, M., Adams, P. J., Artaxo, P., Bahadur, R.,
606 Balkanski, Y., Bauer, S. E., Bellouin, N., Benedetti, A., Bergman, T., Berntsen, T. K.,
607 Beukes, J. P., Bian, H., Carslaw, K. S., Chin, M., Curci, G., Diehl, T., Easter, R. C., Ghan, S.
608 J., Gong, S. L., Hodzic, A., Hoyle, C. R., Iversen, T., Jathar, S., Jimenez, J. L., Kaiser, J. W.,
609 Kirkevåg, A., Koch, D., Kokkola, H., Lee, Y. H., Lin, G., Liu, X., Luo, G., Ma, X., Mann, G.
610 W., Mihalopoulos, N., Morcrette, J.-J., Müller, J.-F., Myhre, G., Myriokefalitakis, S., Ng, N.
611 L., O'Donnell, D., Penner, J. E., Pozzoli, L., Pringle, K. J., Russell, L. M., Schulz, M., Sciare,
612 J., Seland, Ø., Shindell, D. T., Sillman, S., Skeie, R. B., Spracklen, D., Stavrou, T.,
613 Steenrod, S. D., Takemura, T., Tiitta, P., Tilmes, S., Tost, H., van Noije, T., van Zyl, P. G.,



- 614 von Salzen, K., Yu, F., Wang, Z., Wang, Z., Zaveri, R. A., Zhang, H., Zhang, K., Zhang, Q.
615 and Zhang, X.: The AeroCom evaluation and intercomparison of organic aerosol in global
616 models, *Atmos. Chem. Phys.*, 14(19), 10845–10895, doi:10.5194/acp-14-10845-2014, 2014.
- 617 Tsimpidi, A. P., Karydis, V. A., Zavala, M., Lei, W., Molina, L., Ulbrich, I. M., Jimenez, J. L.
618 and Pandis, S. N.: Evaluation of the volatility basis-set approach for the simulation of organic
619 aerosol formation in the Mexico City metropolitan area, *Atmos. Chem. Phys.*, 10, 525–546,
620 2010.
- 621 Vaughan, A. R., Lee, J. D., Misztal, P. K., Metzger, S., Shaw, M. D., Lewis, A. C., Purvis, R.
622 M., Carslaw, D. C., Goldstein, A. H., Hewitt, C. N., Davison, B., Beevers, S. D. and Karl, T.
623 G.: Spatially resolved flux measurements of NO_x from London suggest significantly higher
624 emissions than predicted by inventories, *Faraday Discuss*, doi:10.1039/C5FD00170F, 2016.
- 625 Woody, M. C., Baker, K. R., Hayes, P. L., Jimenez, J. L., Koo, B. and Pye, H. O. T.:
626 Understanding sources of organic aerosol during CalNex-2010 using the CMAQ-VBS,
627 *Atmos. Chem. Phys.*, 16(6), 4081–4100, doi:10.5194/acp-16-4081-2016, 2016.
- 628 Yarwood, G.: Updates to the Carbon Bond Chemical 852 Mechanism: CB05, 2005.
- 629 Young, D. E., Allan, J. D., Williams, P. I., Green, D. C., Flynn, M. J., Harrison, R. M., Yin,
630 J., Gallagher, M. W. and Coe, H.: Investigating the annual behaviour of submicron secondary
631 inorganic and organic aerosols in London, *Atmos. Chem. Phys.*, 15(11), 6351–6366,
632 doi:10.5194/acp-15-6351-2015, 2015.
- 633
- 634

635 **4 Tables and Figures**

636

637 Table 1. Statistics of OA for the VBS_BC_NEW case for February-March 2009 at each AMS

638 site as well as an average of all sites for both VBS_BC_NEW and VBS_BC. Bold numbers

639 represent the stations where model performance criteria were met.

Site*	Mean observed OA ($\mu\text{g m}^{-3}$)	Mean modelled OA ($\mu\text{g m}^{-3}$)	MB ($\mu\text{g m}^{-3}$)	ME ($\mu\text{g m}^{-3}$)	MFB [-]	MFE [-]	r	R ²
Barcelona (BCN)	8.3	5.1	-3.1	3.7	-0.4	0.5	0.6	0.4
Cabauw (CBW)	1.2	1.5	0.3	0.7	0.1	0.5	0.7	0.4
Chilbolton (CHL)	2.4	1.0	-1.4	1.5	-0.9	0.9	0.8	0.6
Helsinki (HEL)	2.7	3.6	0.9	1.8	0.3	0.6	0.3	0.1
Hyytiälä (SMR)	1.3	1.7	0.3	0.8	-0.1	0.6	0.8	0.6
Mace Head (MHD)	0.8	0.7	-0.1	0.3	-0.1	0.7	0.7	0.5
Melpitz (MPZ)	1.5	0.8	-0.6	0.9	-0.6	0.7	0.6	0.3
Montseny (MSY)	3.1	3.5	0.4	2.0	0.1	0.6	0.4	0.1
Payerne (PAY)	4.1	2.9	-1.2	1.9	-0.5	0.7	0.7	0.4
Puy de Dôme (PDD)	0.6	1.1	0.4	0.8	0.3	0.8	0.4	0.2
Vavihill (VAV)	3.9	2.1	-1.8	2.0	-0.8	0.8	0.8	0.6
VBS_BC_NEW	3.0	2.3	-0.7	1.6	-0.3	0.7	0.8	0.6
VBS_BC (Ciarelli et al., 2016a)	3.0	1.4	-1.5	1.8	-0.6	0.8	0.8	0.6

640 * Model OA concentrations extracted at surface level except for the stations of Puy de Dôme

641 and Montseny.

642

643



644 Table 2. Statistics of POA for the VBS_BC_NEW case for February-March 2009 at each
 645 AMS site as well as an average of all sites for both VBS_BC_NEW and VBS_BC. Bold
 646 numbers represent the stations where model performance criteria were met.

Site	Mean observed POA ($\mu\text{g m}^{-3}$)	Mean modelled POA ($\mu\text{g m}^{-3}$)	MB ($\mu\text{g m}^{-3}$)	ME ($\mu\text{g m}^{-3}$)	MFB [-]	MFE [-]	r	R ²
Barcelona	4.0	2.0	-2.1	2.4	-0.5	0.7	0.4	0.2
Cabauw	0.4	0.9	0.5	0.5	0.8	0.9	0.5	0.2
Chilbolton	1.0	0.5	-0.5	0.5	-0.6	0.7	0.8	0.6
Helsinki	0.8	2.5	1.7	1.7	1.0	1.0	0.2	0.0
Hyytiälä	0.1	0.5	0.4	0.4	1.3	1.3	0.5	0.3
Mace Head	0.2	0.1	-0.1	0.2	0.5	1.0	0.2	0.1
Melpitz	0.3	0.3	0.1	0.2	0.3	0.7	0.5	0.2
Montseny	0.5	0.4	0.0	0.3	0.2	0.7	0.3	0.1
Payerne	0.7	1.1	0.3	0.6	0.5	0.7	0.5	0.3
Puy de Dôme	0.2	0.3	0.1	0.2	0.5	0.9	0.2	0.1
Vavihill	1.1	1.0	-0.1	0.6	-0.3	0.7	0.5	0.2
VBS_BC_NEW	0.9	0.9	-0.1	0.7	0.3	0.8	0.6	0.3
VBS_BC (Ciarelli et al., 2016a)	0.9	0.9	0.0	0.8	0.3	0.8	0.6	0.4

647

648

649

650

651

652

653

654



655 Table 3. Statistics of SOA for the VBS_BC_NEW case for February-March 2009 at each
 656 AMS site as well as an average of all sites for both VBS_BC_NEW and VBS_BC. Bold
 657 number represents the stations were model performance criteria were met.

Site	Mean observed SOA ($\mu\text{g m}^{-3}$)	Mean modelled SOA ($\mu\text{g m}^{-3}$)	MB ($\mu\text{g m}^{-3}$)	ME ($\mu\text{g m}^{-3}$)	MFB [-]	MFE [-]	r	R ²
Barcelona	4.4	3.2	-1.2	1.6	-0.4	0.5	0.7	0.5
Cabauw	1.0	0.6	-0.4	0.6	-0.7	0.9	0.7	0.4
Chilbolton	1.4	0.5	-0.9	1.0	-1.1	1.2	0.7	0.5
Helsinki	1.8	1.1	-0.7	1.1	-0.7	0.9	0.4	0.2
Hyytiälä	1.2	1.1	-0.1	0.7	-0.7	1.0	0.8	0.6
Mace Head	0.4	0.5	0.2	0.6	0.3	1.0	0.4	0.2
Melpitz	1.2	0.5	-0.7	0.8	-1.0	1.1	0.6	0.4
Montseny	2.6	3.1	0.5	1.8	0.0	0.7	0.4	0.1
Payerne	3.7	2.0	-1.7	2.1	-0.8	0.9	0.5	0.3
Puy de Dôme	0.6	0.9	0.3	0.8	0.2	0.9	0.2	0.1
Vavihill	2.8	1.1	-1.7	1.7	-1.2	1.2	0.8	0.7
VBS_BC_NEW	2.1	1.4	-0.6	1.2	-0.6	0.9	0.7	0.5
VBS_BC (Ciarelli et al., 2016a)	2.1	0.5	-1.5	1.6	-1.1	1.3	0.7	0.6

658

659

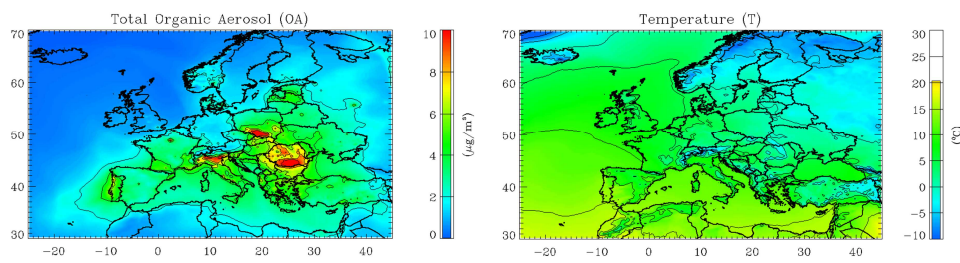
660

661

662

663

664

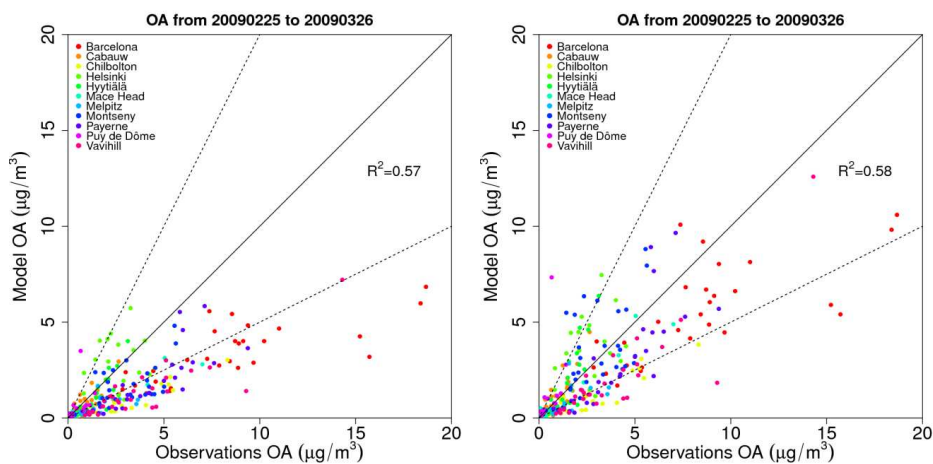


665

666 Figure 1. Modelled average total organic aerosol (OA) concentrations (VBC_BC_NEW) and
667 surface temperature (T) for the period between 25 February and 26 March 2009.

668

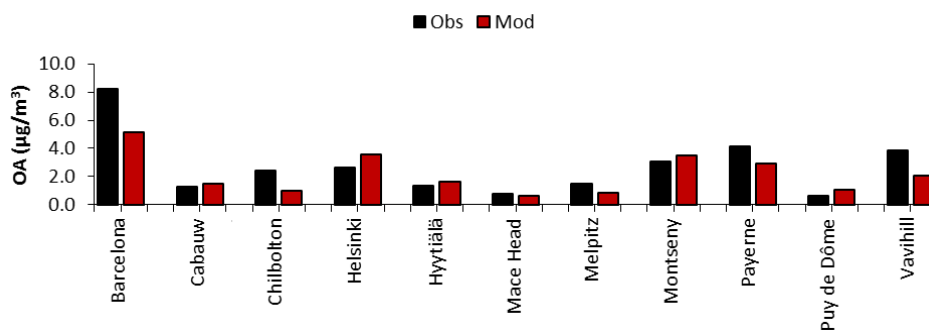
669



670

671 Figure 2. Daily average scatter plots for OA concentrations at 11 AMS sites for the period
672 between 25 February and 26 March 2009 for VBS_BC (left) and VBS_BC_NEW case (right).
673 Solid lines indicate the 1:1 line. Dotted lines are the 1:2 and 2:1 lines.

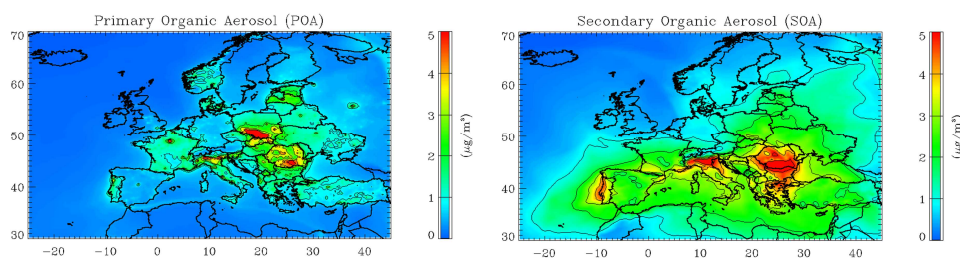
674



675

676 Figure 3. Observed (black) and modelled (VBS_BC_NEW) (red) average OA mass at AMS
677 sites for the period between 25 February and 26 March 2009.

678



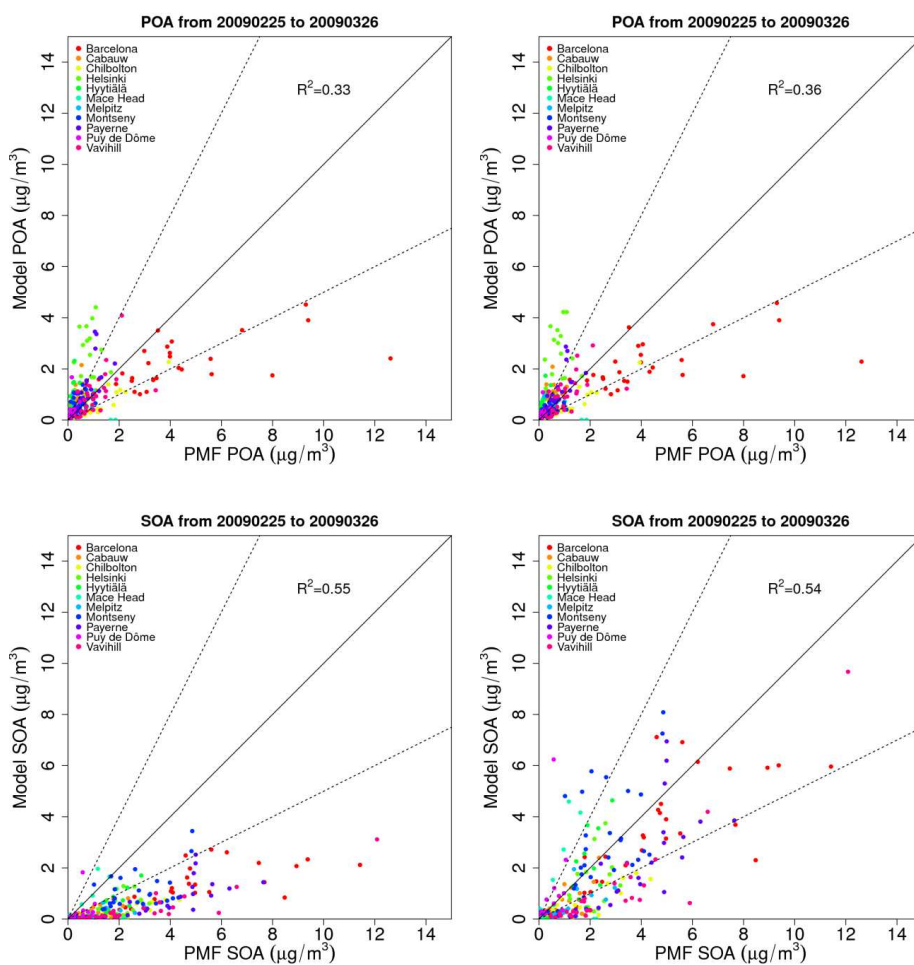
679

680 Figure 4. Modelled average POA (left) and SOA (right) concentrations for the period between
681 25 February and 26 March 2009.

682

683

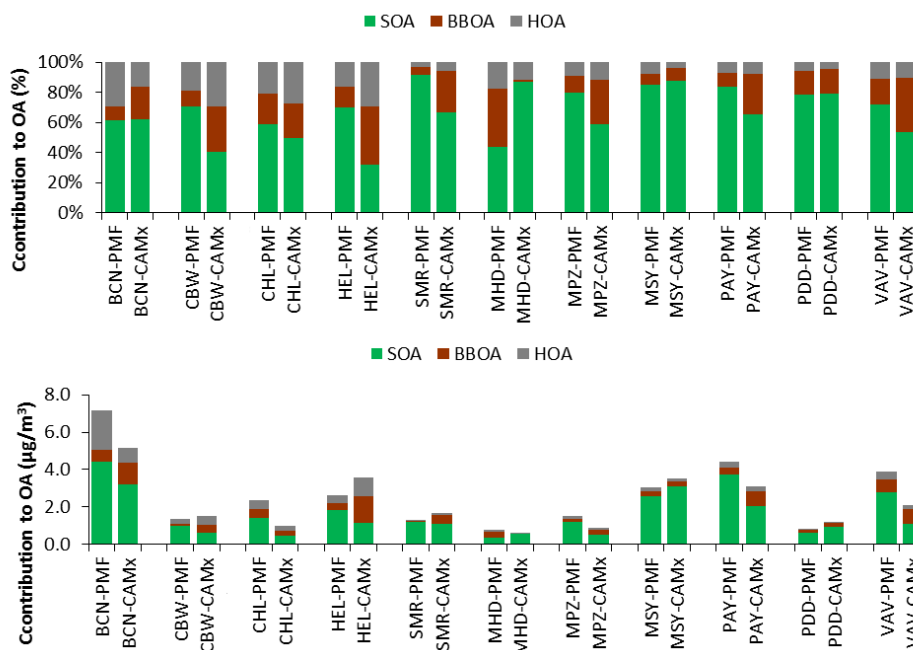
684



685

686

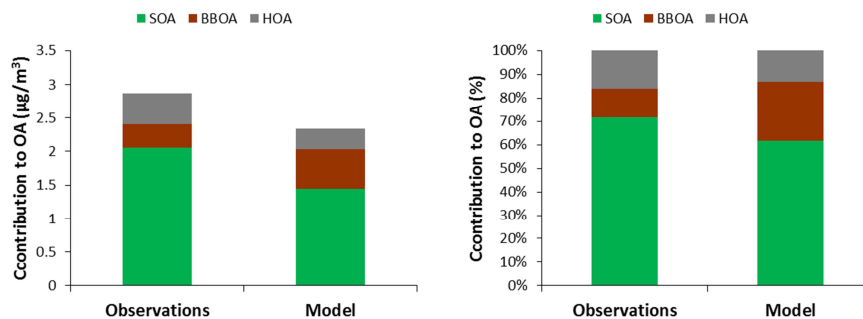
687 Figure 5. Daily average scatter plots of POA and SOA concentrations at 11 AMS sites for
688 February-March 2009 in VBS_BC (Ciarelli et al., 2016a) (left) and VBS_BC_NEW (right).
689 Solid lines indicate the 1:1 line. Dotted lines are the 1:2 and 2:1 lines.



690

691

692 Figure 6. Relative (upper panel) and absolute (lower panel) contribution of HOA, BBOA and
 693 SOA to OA concentrations at 11 sites from PMF analysis of AMS measurements (first bar)
 694 and CAMx VBS_BC_NEW results (second bar) for the period between 25 February and 26
 695 March 2009.

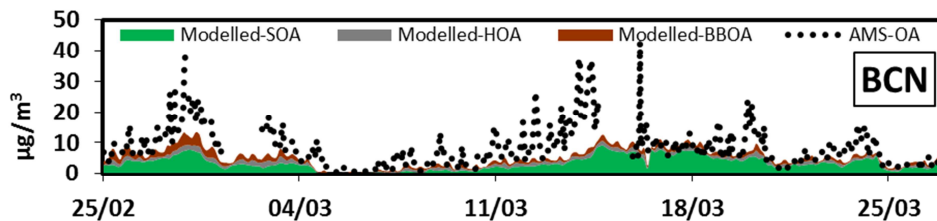


696

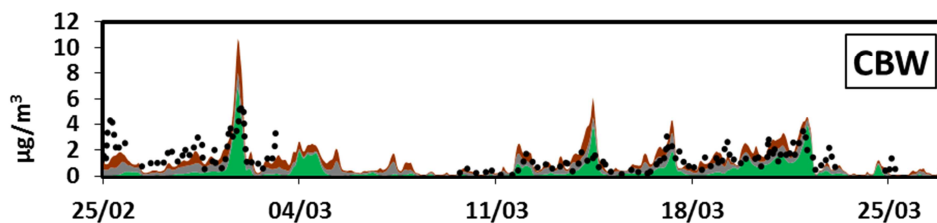
697 Figure 7. Measured and modelled average absolute (left panel) and relative (right panel)
 698 contributions of HOA, BBOA and SOA to OA concentrations for all the 11 sites for the
 699 period between 25 February and 26 March 2009.



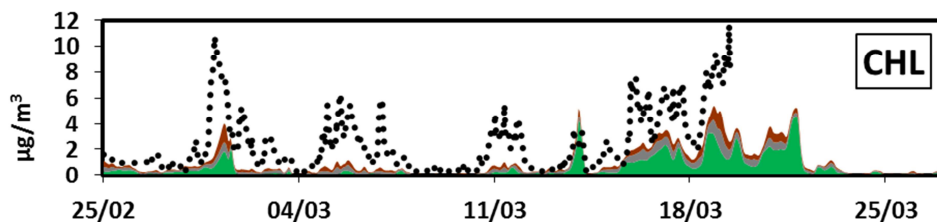
700



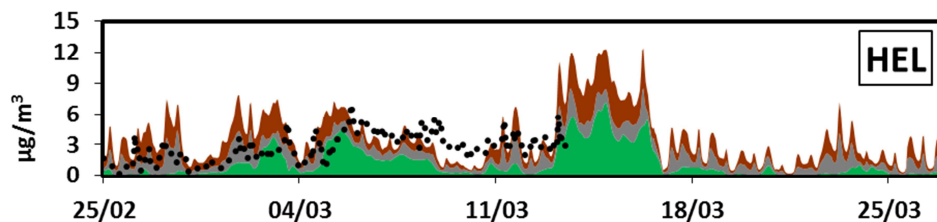
701



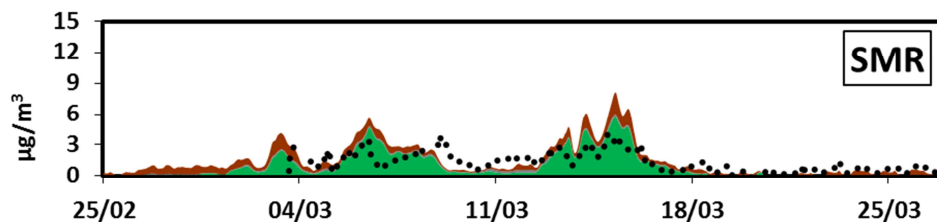
702



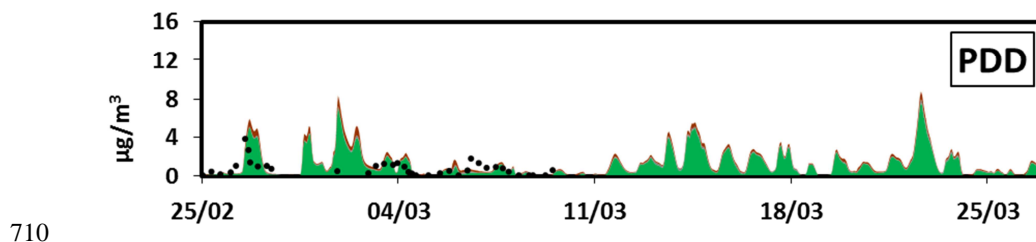
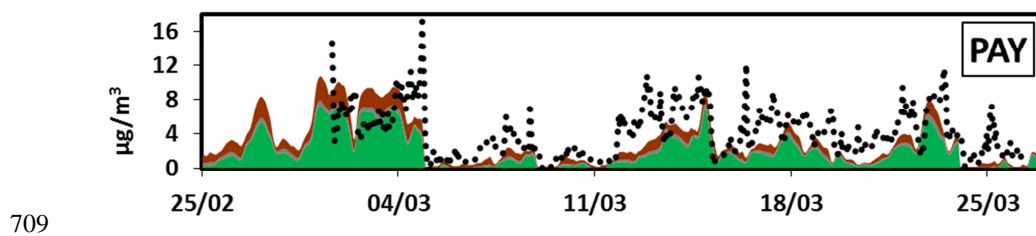
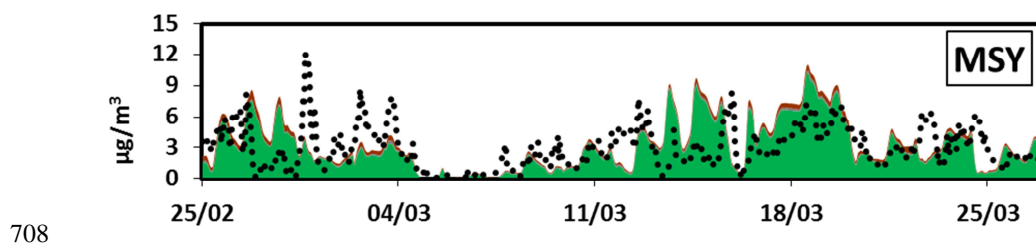
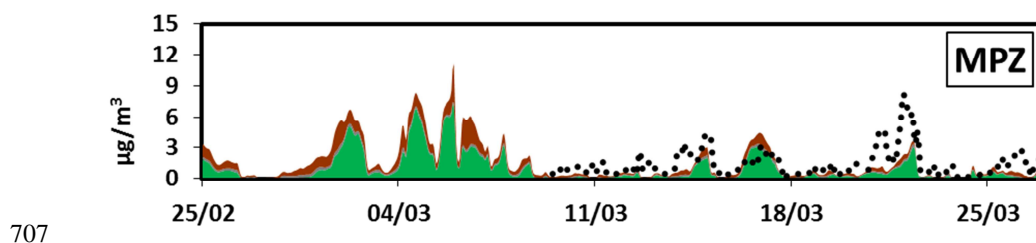
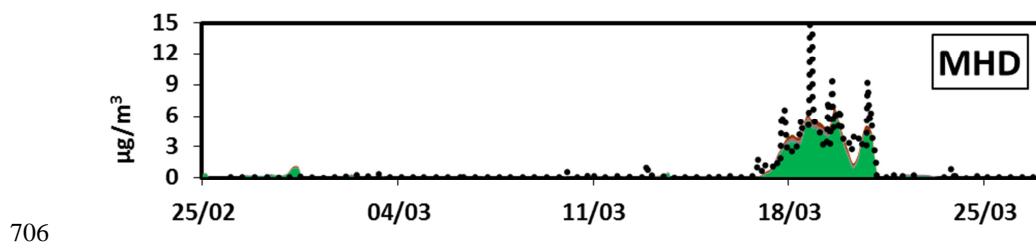
703

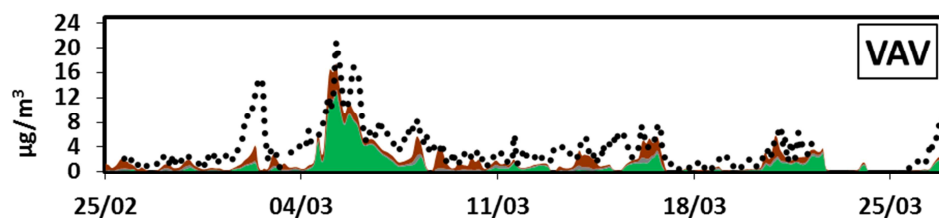


704



705

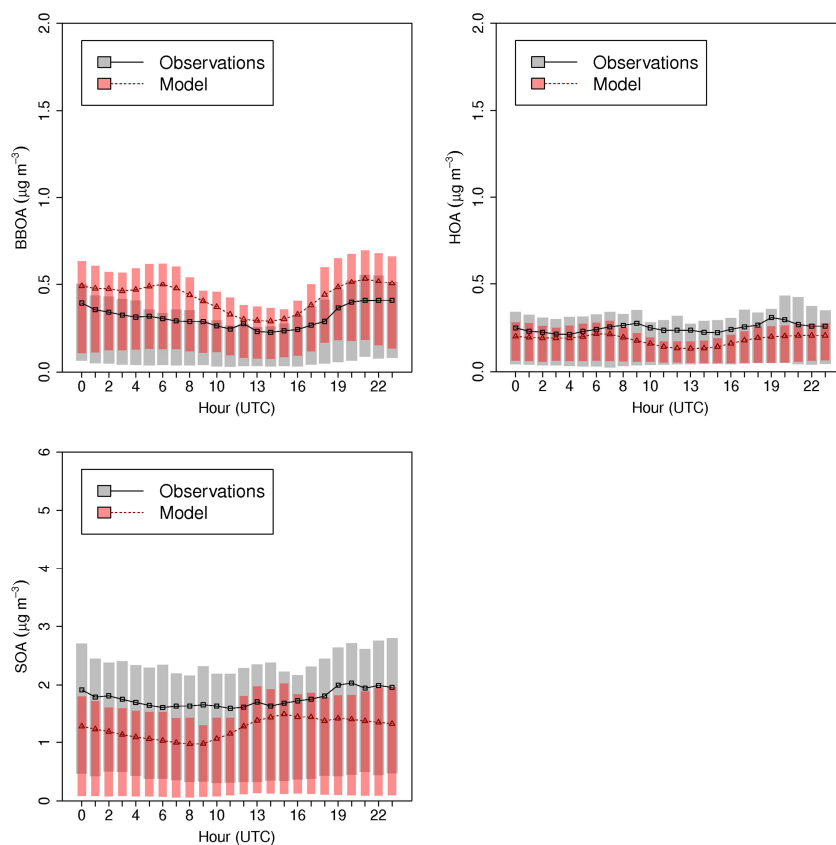




711

712 Figure 8. Comparison of measured hourly OA mass concentrations (AMS-OA dotted line),
713 with modelled components HOA, BBOA and SOA.

714



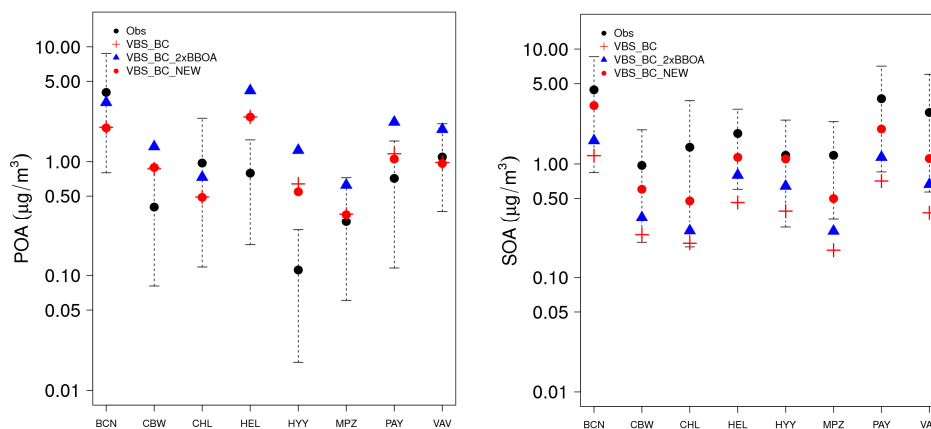
715

716

717 Figure 9. Comparison of modelled (red) and measured (grey) BBOA, HOA and SOA diurnal
718 profiles at the rural-background sites. The extent of the bars indicates the 25th and 75th
719 percentiles.



720

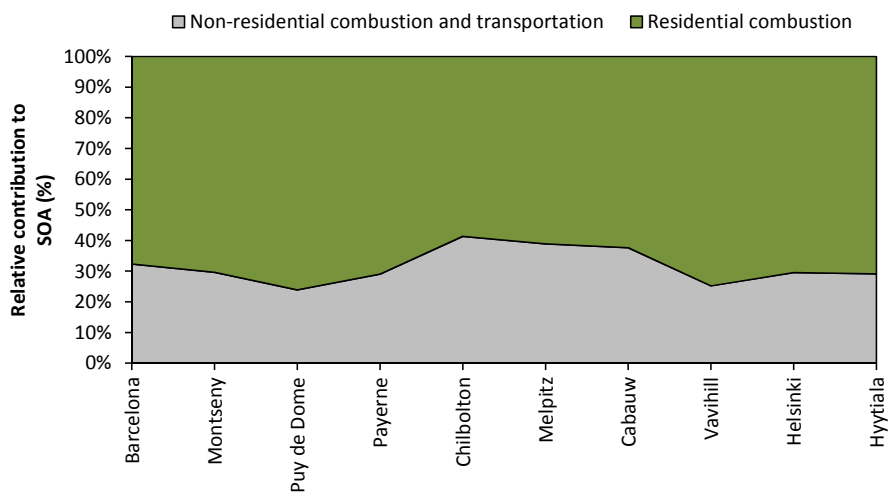


721

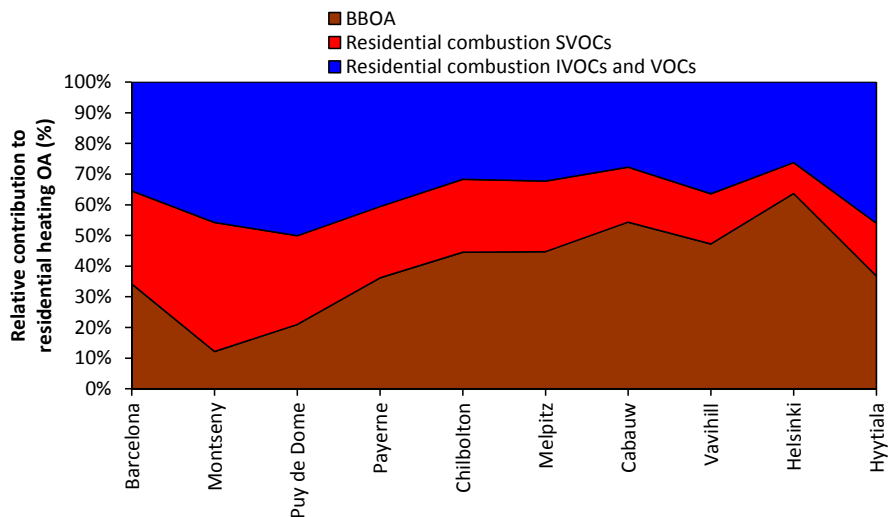
722

723 Figure 10. POA (left) and SOA (right) average concentrations at 8 AMS sites for February-
724 March 2009 in the VBS_BC , VBS_BC_2xBBOA and VBS_BC_NEW cases. Dotted lines
725 indicate the 10th and 90th quartile range. Data for the Puy de Dôme and Montseny sites at
726 higher layers are not available for the VBS_BC_2xBBOA scenario.

727

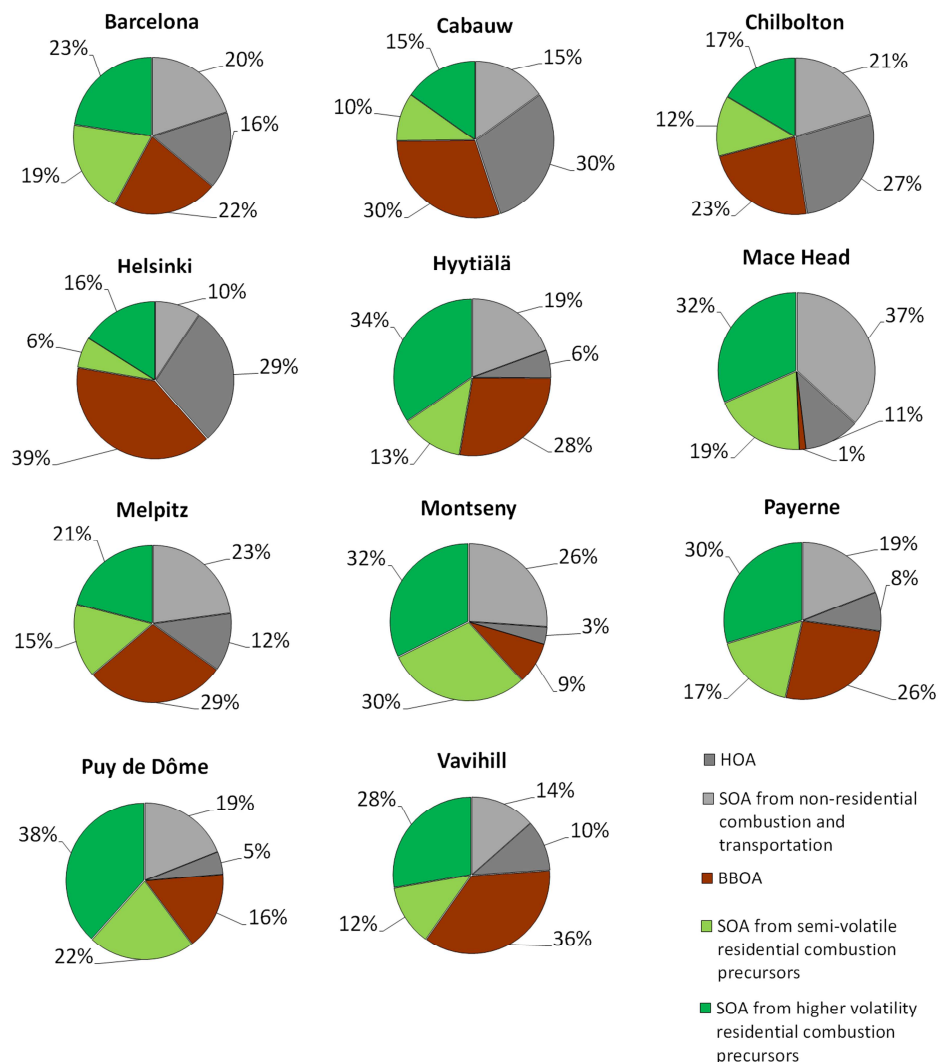


728



729

730 Figure 11. Contribution of residential and non-residential combustion precursors to SOA at
731 different sites (upper panel). Contribution of BBOA, SVOCs and higher volatility organic
732 precursors to residential heating OA (lower panel). Stations are ordered from south to north.



733

734 Figure 12. Average modelled composition of OA at the 11 AMS sites for the period between
 735 25 February and 26 March 2009.